Peer-reviewed version available at *J. Clin. Med.* **2020**, *9*, 1473; doi:10.3390/jcm9051473

Article

Highly Conserved Homotrimer Cavity Formed by the SARS-CoV-2 Spike Glycoprotein: A Novel Binding Site

Umesh Kalathiya*[1], Monikaben Padariya[1], Marcos Mayordomo[1], Małgorzata Lisowska[1], Judith Nicholson[2], Ashita Singh[1], Maciej Baginski[3], Robin Fahraeus[1], Neil Carragher[4], Kathryn Ball[4], Juergen Hass[5], Alison Daniels[5], Ted R. Hupp*[1,4], Javier Antonio Alfaro*[1,4]

[1] International Centre for Cancer Vaccine Science, University of Gdansk, Wita Stwosza 63, 80-308 Gdansk, Poland
[2] Sharp Life Science (EU) Limited, Oxford Science Park, Edmund Halley Rd, Oxford OX4 4GB, England, United Kingdom
[3] Department of Pharmaceutical Technology and Biochemistry, Faculty of Chemistry, Gdansk University of Technology, Narutowicza St 11/12, 80-233, Gdansk, Poland
[4] Institute of Genetics and Molecular Medicine, University of Edinburgh, Edinburgh, Scotland EH4 2XR, United Kingdom
[5] Department of Infectious Disease, Edinburgh, Scotland EH4 2XR, United Kingdom
* Correspondence: umesh.kalathiya@ug.edu.pl (U.K), ted.hupp@ed.ac.uk (T.R.H.), javier.alfaro@proteogenomics.ca (J.A. A.)

Abstract: An important stage in SARS-CoV-2 life cycle is the fusion of spike(S) protein with the ACE2 host-cell receptor. Therefore, to explore conserved features in S protein dynamics and to identify potentially novel regions for drugging, we measured variability derived from 791 viral genomes and studied its properties by MD simulation. The findings indicated that S2 subunit (HR1, CH, and CD domains) showed low variability, low fluctuations in MD, and displayed a trimer cavity. By contrast, the RBD domain, which is typically targeted in drug discovery programmes, exhibits more sequence variability and flexibility. Interpretations from MD suggest that the monomer is in constant motion showing transitions up-to-down state, and the trimer cavity may function as a 'bouncing spring' that may facilitates S protein interactions with ACE2. Feasibility of trimer cavity for potential drug target was examined by SBVS screening. Several hits that have already been validated or suggested to inhibit the SARS-CoV-2 virus in cell systems were identified; in particular, the data suggest an action mechanism for such molecules including Chitosan and macrolide types. These findings identify a novel binding-site formed by the S protein, that might assist in future drug discovery programmes aimed at targeting the CoV family of viruses.

Keywords: SARS-CoV-2; COVID-19; spike glycoprotein; variability; molecular docking; molecular dynamics; inhibitors

1. Introduction

The global pandemic developing from December 2019 by a strain of severe acute respiratory syndrome coronavirus 2 (SARS-CoV-2) can cause COVID-19 disease. This emergent variant adds to the additional coronavirus strains that can infect humans including HCoV-OC43, HCoV-HKU, SARS-CoV, HCoV-229E, hCoV-NL63, and MERS-CoV[1-5, 6]. Coronaviruses (CoVs) are positive-sense, enveloped, single-stranded RNA viruses that are classified taxonomically as a family *Coronavirdiae* and order *Nidovirales* [4]. There are four genera of CoVs, including αCoV, βCoV, δCoV, and γCoV; most δCoVs and γCoVs target avians whilst αCoVs and βCoVs infect rodents and bats [1, 7, 8]. Severe acute respiratory syndrome CoV (SARS-CoV) outbreaks have also emerged previously creating an

epidemic [2, 4, 9-13]. Although the mortality of MERS-CoV, SARS-CoV, and SARS-CoV-2 is substantial, there are no preventative vaccines or drugs available to treat patients infected with the virus [9, 11, 12]. The current public health emergency of international concern (PHEIC; by the World Health Organization) has declared SARS-CoV-2 (COVID-19; a novel βCoV) as a pandemic threat. The data obtained from WHO (22/April/2020) suggest that the virus has caused 2,471,136 infections, 169,006 deaths, and it has affected over 200 countries.

COVID-19 encodes for Open Reading Frame 1ab (ORF1ab), of which so far three proteins are broadly recognized as drug targets, since they are crucial components for infections and progression: the SARS-CoV-2 protease [14, 15], RNA-dependent RNA Polymerase (RdRP) [14, 16, 17], and SARS-CoV-2 spike glycoprotein (S protein) [15,18-20]. The SARS-CoV-2 protease processes the polyproteins that are translated from the viral RNA, and it has been heavily studied using small molecules inhibitors [15]. To penetrate the host, the SARS-CoV-2 (COVID-19) makes use of homotrimeric class I glycosylated fusion spike (S) protein [18, 21, 22]. Fusion of the viral and host cell membranes is facilitated by the spike glycoprotein, which undergoes a significant conformational change within its structures [18, 21, 22].

SARS-CoV-2 studies suggest [18, 23, 24] that the spike glycoprotein functions as a homotrimer. The recognition and subsequently fusion of two membranes from the virus and the host is triggered by the S1 subunit, which binds the host cell receptor: angiotensin-converting enzyme 2 (ACE2) [16, 25-31]. Several insights from structural biology are consistent with the role for this domain in affecting the infection rate of the virus. This host-virus interaction is mediated by the receptor binding domain (RBD) domain from S1 subunit of SARS-CoV-2 spike glycoprotein that forms a hinge-like conformation [18, 32], i.e., 'down' and 'up' states that represents the host cell receptor-inaccessible and receptor-accessible [18]. This receptor-accessible 'up' conformation exists in a highly fluctuating state [33-36]. Binding to the host target destabilizes the pre-fusion homotrimer, which sheds off the S1 subunit, and allows for the transition of the S2 subunit to a highly stable postfusion conformation [18]. Interestingly, protein-mediated cell-cell fusion assays suggest that SARS-CoV-2 S protein displays an elevated plasma membrane fusion capacity when compared to that of SARS-CoV [32, 37].

Several studies have aimed to define the mechanism of binding of SARS-CoV-2 to the host cell receptor [38]. Molecular dynamics simulations of the spike(RBD)-ACE2 complex over 10 ns indicated that RBD-ACE2 binding free energy for SARS-CoV-2 is better than the SARS-CoV [39]. Similarly, other studies have shown that the SARS-CoV-2 S protein has a better binding affinity to ACE2 at two different "up" angles of the RBD than SARS-CoV [40]. Structural features at the S protein-ACE2 interface suggest that RBD domain residues Q493 and P499 are responsible for maintaining protein-protein stability [41]. Using a virtual high-throughput screening approach, small-molecules have been identified that can interact either with the SARS-CoV-2 S protein at its host receptor region or the ACE2 interface (i.e. RBD domain) [42]. Natural compounds present in Curcuma sp., *Citrus* sp., *Alpinia galanga*, and *Caesalpinia sappan* could target the RBD domain of the SARS-CoV-2 spike glycoprotein, the protease domain (PD from ACE2), and the SARS-CoV-2 protease [20]. A set of B cell and T cell epitopes derived from the spike (S) and nucleocapsid (N) proteins that map identically to SARS-CoV-2 proteins were identified as potential vaccine candidates [23].

Applying an integrative, antiviral drug repurposing methodology, the interplay between the CoV-host interactome and drug targets in the human protein-protein interaction network have been defined [43]. Bioinformatics methodologies were used to identify neutralizing antibodies that might interact with interfaces formed by the spike glycoprotein and host cell receptor [24]. By targeting the RBD domain of the spike glycoprotein protein using receptor docking experiments, Kanishka *et al.* identified small molecule inhibitors [44]. In the majority of studies, the most common strategy is focused on targeting the interface formed by SARS-CoV-2 spike glycoprotein and the host cell receptor (i.e. RBD-ACE2). Currently there are no robust drugs for wide-spread dissemination available against coronaviruses including SARS-CoV-2 (COVID-19). Due to the relatively rapid spread in the current outbreak and the relatively high mortality rate (3.5%), more rapid development of new or repurposed antiviral drugs is of high value. Although the majority of drug discovery programmes target classically druggable enzymes encoded by the virus, such as the viral RNA

polymerase inhibited by remdesivir [13, 17, 45], there is a paucity of information concerning the other regions of spike glycoprotein outwith the ACE2-binding domains, especially the domains interacting with the viral membrane.

The SARS-CoV-2 (COVID-19) is a homotrimer composed of three subunits. Each monomeric protein contains an N-terminal ACE2 binding domain (receptor binding domain; RBD), a central helix/heptad repeat, and a C-terminal region that interacts with the plasma membrane [18]. Homotrimer S protein assembly from monomeric forms can be rate limiting in cells, suggesting a possible space for intervention on the S protein-dependent viral life cycle [46]. Our current study focuses on understanding the variability of the spike glycoprotein trimer in SARS-CoV-2 with respect to the strains from other viral genomes and identifying the changes in the molecular properties due to conformational flexibility in the spike glycoprotein trimer from SARS-CoV-2. This information was used to identify potentially novel drug pockets or the active site regions specifically in the oligomeric SARS-CoV-2 spike glycoprotein.

We performed molecular dynamic simulations (MDS) of the monomeric and trimeric form of the SARS-CoV-2 spike glycoprotein, and developed a virtual screening using a FDA-approved chemical library. We identified and focused on an apparent cavity formed by three subunits (the homotrimer) that our simulations suggest form dynamic movements that mimic a 'bouncing spring' or a 'sarrus linkage (converting a circular motion to a linear motion or vice versa)' when interacting with the host cell receptor (ACE2). This motion might be important in the fusion of virion and the host cell membrane. We hypothesized such a cavity formed by three chains (A, B, and C) might form an acceptor for small molecules and we asked whether small molecules could be identified using simulations with a relatively high binding energy. We identified several known compounds with predicted binding energy of GBVI/WSA dG(kcal/mol) from -35 to -71, some of which are already in clinical trials including Sirolimus (Rapamycin; a macrolide type; NCT03901001 not yet recruiting) [47-49] and Ritonavir (open-label trial in hospitalized adults with severe COVID-19) [48, 50-52]. In addition, one of the top hits we have identified, Chitosan, has a recently reported derivative inhibiting SARS-CoV-2 coronavirus replication in cell lines [53, 54]. A previous study has also shown that the chitosan derivatives can interact with the Spike protein and block its interaction with the host receptor [55]. Our data suggest a mechanism whereby Chitosan (and possibly its derivatives), as well as macrolide type molecules, could bind to a pocket formed by the S protein trimer and provides a novel domain to focus on for future drug discovery projects.

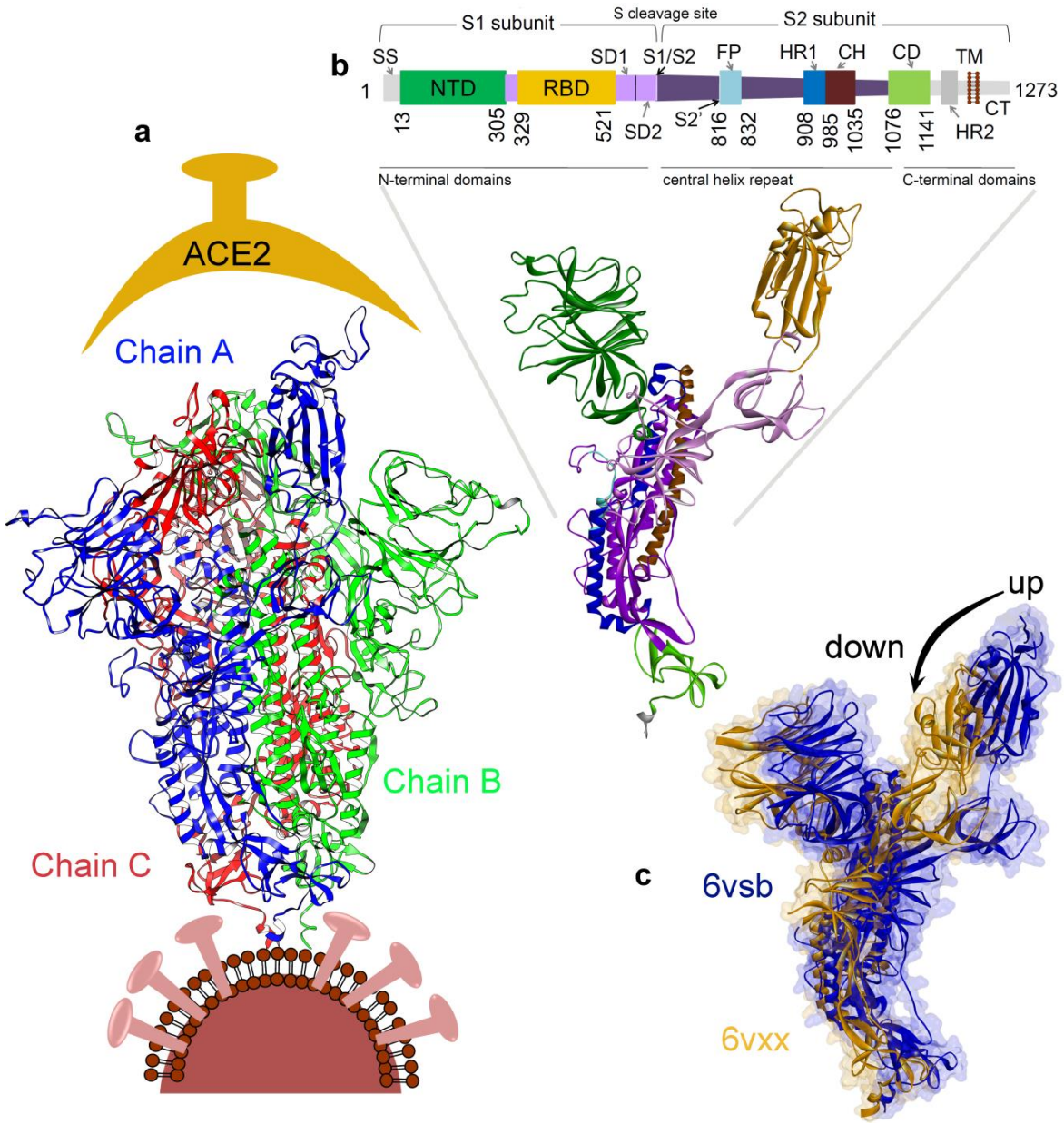

Figure 1. SARS-CoV-2 structure and function. (a) The SARS-CoV-2 (COVID-19) spike (S) glycoprotein (PDB: 6vsb) [18]. (b) Domain structure of the S protein. signal sequence (SS), the N-terminal domain (NTD), receptor-binding domain (RBD), subdomain 1 and 2 (SD1&2), protease cleavage sites (S1/S2/S2'), fusion peptide (FP), heptad repeat 1 and 2 (HR1&2), central helix (CH), connector domain (CD), transmembrane domain (TM), cytoplasmic tail (CT) [18, 19]. (c) Receptor-binding domain illustrating the "up or open" (PDB: 6vsb [18]) and "down or closed" (PDB: 6vxx [31]) conformation of the RBD domain.

2. Material and Methods

2.1. Bioinformatics analysis of SARS-CoV-2 variability

A total of 791 genome viral sequences were downloaded from the Global Initiative on Sharing All Influenza Data platform (GISAID) [56], in order to evaluate the variability of different domains of the spike glycoprotein in SARS-CoV-2. The genomes were selected by first requiring high coverage and complete sequences. Further filtering was applied to obtain complete sequences on the targeted domains reducing the total number of strains to 768. Total protein sequences were acquired from 3 frame translation using the transeq tool from EMBOSS package (version 6.5.7) [57]. The amino acid

chains from the spike glycoprotein were aligned to the reference protein (PDB ID: 6vsb [18, 58]) using MUSCLE [59]. Variations in the amino acid or the residue changes were scanned on the entire S protein sequence, along with two areas of interest in the multiple alignment file, focusing a subset of the S2 subunit (the HR1, CH and CD regions) and the RBD domain (Figure 1 and Tables S1, S2, S3).

2.2. Structural bioinformatics, molecular dynamics

The Cryo-EM homotrimer structure of SARS-CoV-2 spike glycoprotein was retrieved from the Protein Data Bank (http://www.rcsb.org/pdb; PDB ID: 6vsb; Figure 1) [18, 58]. In addition, the missing amino acids (residues range: 67-78, 96-98, 143-155, 177-186, 247-260, 329-334, 444-448, 455-490, 501-502, 621-639, 673-686, 812-814, and 829-852) coordinates in the structure of SARS-CoV-2 spike glycoprotein were built using the swissmodel (Figure 1) [60]. Molecular dynamics simulations (MD) were carried on the model systems as per standardized pipelines [61-63] (detailed method explained in the supplementary materials). The GROMACS 4.6.5 [64] program (GROMACS; Groningen Machine for Chemical Simulations) was used to perform MD calculations assigning the CHARMM27 forcefield [65]. We performed 100 ns molecular dynamics simulations on two systems: (i) monomeric protein and (ii) the homotrimer of the spike glycoprotein. In our analysis of the MD simulation, the dynamics of the monomer S protein serves as control to the homotrimer, which is the functional unit. Initially the model systems were energy minimized, which provides a base-line model structure and resolves poorly resolved conformations often found in crystal structures [13, 18, 61, 66-69]. A simulation box of solvent atoms is then added to enhance simulation realism. Following that, using the NPT (number of particles (N), system pressure (P), and temperature (T); isobaric-isothermal) thermodynamic ensemble, equilibration of the systems was performed to adjust solvent molecules with counter ions in the simulation box [70]. These equilibrated systems were subsequently used to perform final MD production runs for 100 ns, and results were analysed using GROMACS [55], BIOVIA Discovery Studio [Dassault Systemes, BIOVIA Corp., San Diego, CA, USA], Chimera, and visual molecular dynamics (VMD) tools [70-72].

2.3. In silico drug discovery: SBVS screening

Structure-based virtual screening (SBVS) is an application of *in silico* methods that identify promising lead molecules from chemical libraries or databases. These methods are computational counterparts of experimental biological evaluation methods, such as high-throughput screening (HTS). FDA-approved drug libraries were retrieved from Target Molecule Corp. (TargetMol; www.targetmol.com) and Selleck Chemicals (Selleckchem; www.selleckchem.com) vendors. The SBVS against the SARS-CoV-2 spike glycoprotein was performed using the Molecular Operating Environment (MOE; Chemical Computing Group Inc.) package [73, 74]. Receptor-ligand binding or the docking using the CHARMM27 forcefield [65] was evaluated using GBVI/WSA ΔG scoring function [75], and the compounds showing best energies with the S protein were selected for further analysis. GBVI/WSA ΔG is a forcefield based scoring function which determines the free energy of binding of the ligand from a given pose with respect to the protein [74]. In addition, we have also selected the compounds that showed comparatively stable interactions with the S protein trimer. The receptor-ligand docking was performed using the “Triangle Matcher" placement method, with the receptor as rigid and the ligands as flexible [73, 74].

3. Results

3.1. Investigating the SARS-CoV-2 spike glycoprotein reveals a cavity with potential function as a drug pocket

3.1.1. Variability in the spike glycoprotein

We were interested to define variance in the SARS-COV-2 spike protein. Understanding regions of high and low variance is key to identifying regions that may be functionally conserved and

Preprints (www.preprints.org) | NOT PEER-REVIEWED | Posted: 24 April 2020 doi:10.20944/preprints202004.0439.v1

Peer-reviewed version available at J. Clin. Med. 2020, 9, 1473; doi:10.3390/jcm9051473

potentially important to the virus life cycle or those under positive evolutionary pressure to avoid the immune system.

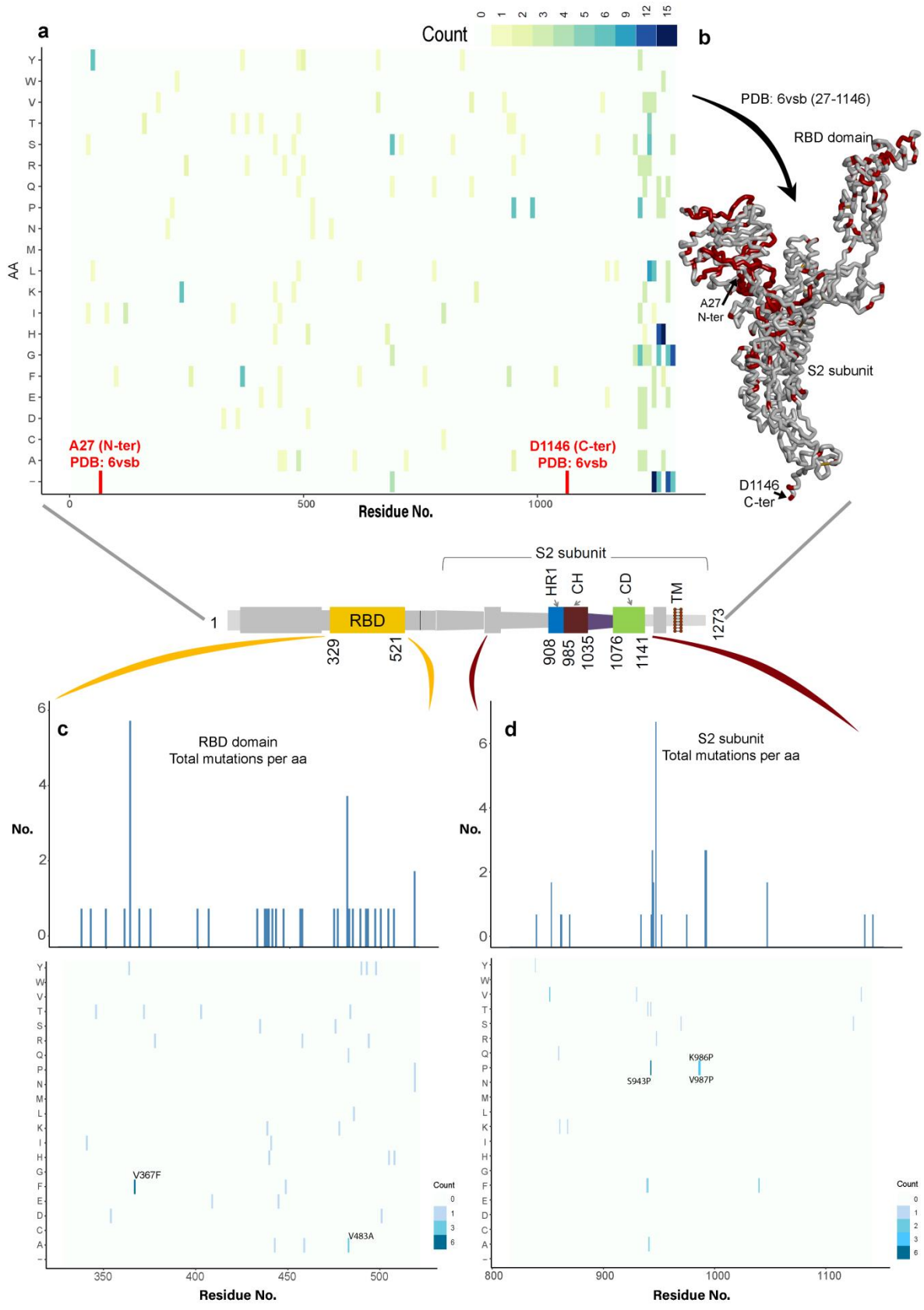

Figure 2. Variability in the SARS-CoV-19 S protein. **(a)** The heat map contains the amino acid substitutions for each position in the spike glycoprotein compared to the consensus sequence (wild-

type) from the alignment of 791 SARS-CoV-2 strains from the GISAID database [56]. (**b)** Represents the previous variations over the S protein structure, marking in red color the spots of variability. (**c** and **d**) Analysis of the amino acid substitutions in the RDB domain and in the S2 subunit (HR1, CH and CD domains), including a bar plot with the total number of changes for each position.

Examining the variability of the S protein in SARS-CoV-2 and its different domains, a total of 791 genome viral sequences were retrieved from the GISAID [56]. A global view of the mutation space of the virus is presented in Figure 2a, which represents the amino acid substitutions in bins of 10 amino-acids across the spike glycoprotein. These hotspots of variation are mostly constrained to the NTD and RBD domain (Figure 1b and 2b), We investigated the variability in the entire sequence of S protein, focusing on the regions that showed low-variability in the structure (Figure 2).

By investigating the variations in the residue changes across the entire S protein sequence or all the regions of lower variability (Figure 2a and Table S1), the S2 subunit exhibited the lowest sequence variability (residue range; 816-1141; Figure 1b and 2c). Moreover, previous studies have identified that the active site region for this S protein is located in the RBD domain which interacts with the host cell receptor, ACE2 [18, 20, 26, 38, 39, 40, 42, 44]. Comparing the variability of the RBD domain (which is targeted for drug designing approaches) and S2 subunit domains, the RBD domain was shown to contain more mutations in its region compared to the HR1, CH and CD domains Figure 2b, 2c, and Table S1, S2, S3, S4). These data suggest mutation by natural selection, the viral-host 'arms race', might operate more frequently on the RBD domain, yet the S2 subunit conservation is suggestive of an important core function. These findings prompted our focus on the S2 subunit as an important region to investigate for drug discovery screens.

3.1.2. Molecular properties and dynamics of the S protein

We next traced the dynamics of different domains in the S protein using MD simulations (Figure 1b). The simulated model systems of the S proteins were first processed to check the stability of protein and simulated systems. The stability of the simulated S protein (in its homotrimer and monomer forms) in the solvent environment was traced by RMSDs (root mean square deviation), a time dependent change in the non-hydrogen atoms (Figure 3a). The RMSD plots (Figure 3a) suggests that the trimer S protein is more stable compared to the monomer, and the chain A in trimer has higher RMSD of ~2 Å compared to the other two chains, a consequence of the fact that the 'up' (or active to bind ACE2) conformation [18] induces flexibility.

The root mean square fluctuations (RMSF) was computed on the C**α** atoms of each residue from the spike protein, in order to trace their flexibility and thereby define the motions of different domains (Figure 3b). The RMSF findings in both forms (monomer and trimer) identified that the amino acids in the RBD domain (residue range: 329-521) of the S protein, were found to be highly fluctuating (Figure 1b and 3b). These analyses correlate with previous studies [33-36, 39], particularly, amino acids 470-490 were found to be highly fluctuating and this region is responsible for interacting with the ACE2 host cell receptor. In addition, examining other regions of the S protein suggest that the S2 subunit domains (residue range 850-1141; HR1, CH, and CD) showed the least fluctuations within the entire protein sequence (Figure 3b). This correlates with the Cryo-EM studies performed on the S protein; that the S2 subunit is more stable [18] compared to the RBD, and that this subunit is responsible for a highly stable postfusion conformation of the S protein [18, 32]. From the perspective of designing drugs, the more stable or less flexible a region in a protein is, the more able we are to trace a better hit molecule. In this case of the spike protein, the RMSF findings guide us towards the S2 subunit (Figure 3b).

Moreover, tracing residues involved in the H-bond interactions between two chains (e.g. chain A-chain B) of the homotrimer, we observed that the RBD domain residues were also involved in intermolecular interactions with each other and with high occupancy (%). This suggests that interactions between chains in the homotrimer might equilibrate the S protein to a 'down' from an 'up' conformation (Figure S1 and Table S5).

Preprints (www.preprints.org) | NOT PEER-REVIEWED | Posted: 24 April 2020 doi:10.20944/preprints202004.0439.v1

Peer-reviewed version available at J. Clin. Med. 2020, 9, 1473; doi:10.3390/jcm9051473

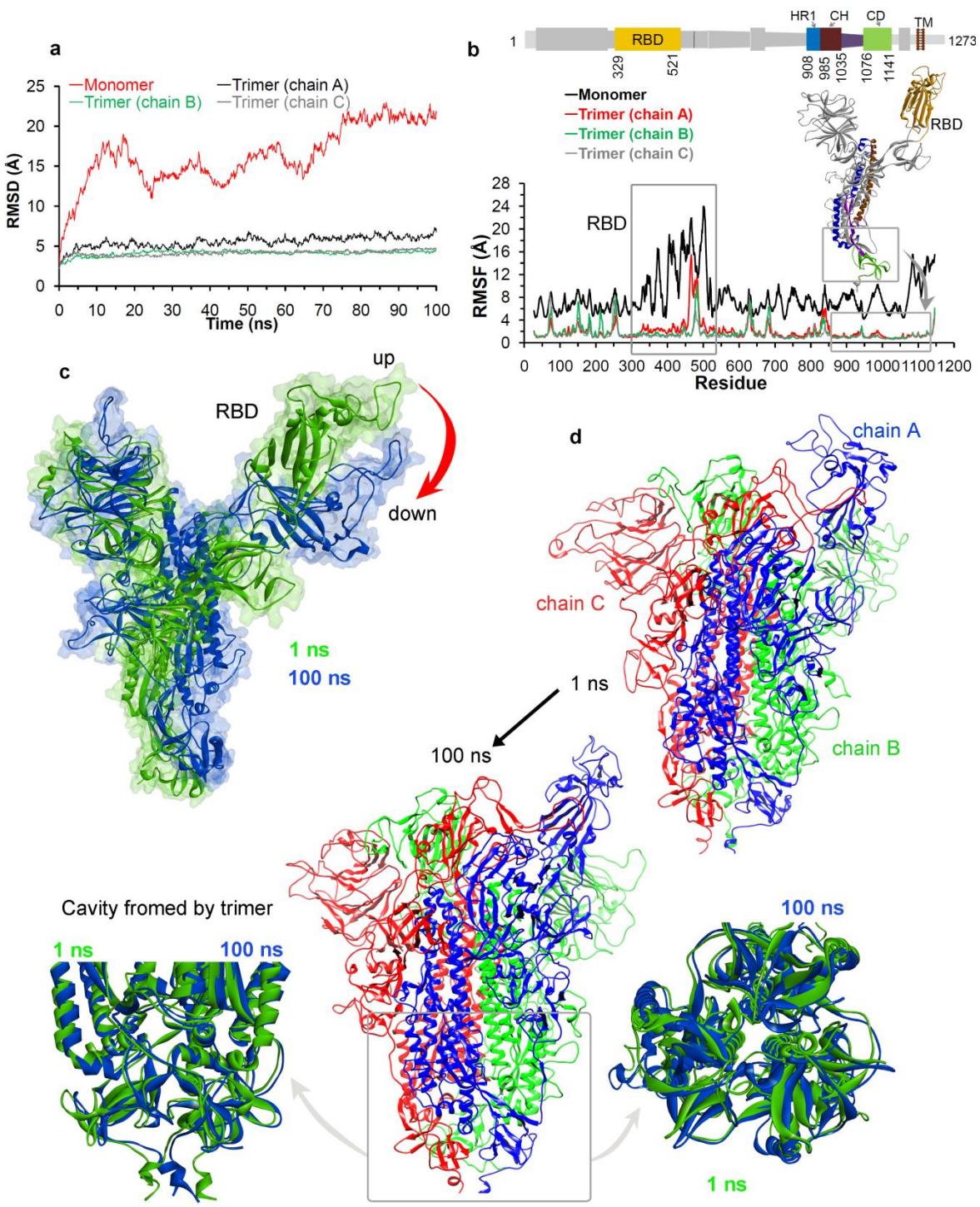

Figure 3. Conformational dynamics of the SARS-CoV-2 spike glycoprotein. **(a** and **b)** RMSD and RMSF of the monomeric and trimeric forms. **(c)** The 'up' and 'down' state traced during the MD simulations of the monomeric form. **(d)** The conformation dynamics of homotrimer S protein, as well as the highlighted cavity formed by the trimer state and its evolution over 100 ns of MD.

The structural dynamics over the time course for S protein in the monomer and the homotrimer form was monitored during MD simulations (Figure 3c and 3d). The monomeric S protein in the solvent environment has obtained a movement from the 'up' active state towards the 'down' inactive state for the RBD domain (Figure 1c, 3c, and Movie S1). These correlate with the previous findings that the RBD domain can form two different conformations, i.e., 'down' and 'up' states, which represents the host cell receptor-inaccessible and receptor-accessible, respectively [33-36]. The SARS-CoV-2 S protein has a better binding affinity to the ACE2 receptor at two different "up" angles of

RBD domain compared to the SARS-CoV [40]. Figure 3c and Movie S1, describes the conformational change in other regions of S protein, when the RBD domain moves towards an up-down state.

Figure 3d and Movie S2 represent the dynamics of the homotrimer S protein, suggesting that the RBD domain of chain A opens more widely in its 'up' state. Domains HR1, CH and CD, close to the viral transmembrane showed the least movement (Figure 3d) during the MD simulations, and exploration of the structural orientation of these domains (Figure 3d and Movie S2) suggest that they form a large pocket or cavity using three chains from a homotrimer S protein. The slight movement observed in homotrimer during MD of this cavity (Movie S1 and S2), and the structural orientation suggest that it could work as 'bouncing spring' or 'sarrus linkage'. One may postulate that, when the S protein interacts with the ACE2 receptor, this 'bouncing spring' or 'sarrus linkage' forms movement may be important in the fusion of virion with the host membrane. Additionally, this cavity from the S protein could work as a platform for the design or development of new drug leads against this protein (Figure 3d). Such molecules might de-stabilize the trimer upon viral entry or upon viral coat assembly. There have been several studies performed to design drugs specific SARS-CoV-2 S protein [20, 38-40, 42, 44], however, most of them are focused on the RBD domain. In addition, from our MD simulation and variability analysis (Figure 2 and 3) it was observed that this RBD domain is highly flexible and variable, therefore, drugging this flexible site may be an obstacle in finding active hit molecules. By targeting the less variable S2 region, such as the cavity formed by the homotrimer (Figure 2 and 3d) we suggest that this might be a novel approach to develop small molecule drug leads.

3.2. Measuring the feasibility of the homotrimer cavity

From our investigation into the genomics of the virus, as well as our findings from MD simulations of the spike protein indicate that a conserved region with significant mechanistic importance may be a trimer cavity or pocket formed by the S2 subunit (HR1, CH and CD domains) in the S protein (Figure 2 and 3). Therefore, we next investigated the targetability of this region or pocket using the MOE (Chemical Computing Group Inc.) package [73, 74], before using it for high-throughput virtual screening (or SBVS) using FDA-approved drugs. The 'Alpha Shapes' construction [74, 76] geometric method was used to compute the possible residues that can be considered for ligand docking from this trimer cavity in S protein (Figure 4a).

High-throughput virtual screening is a powerful computational approach that is increasingly being used in the drug discovery process, through the *in silico* identification of the novel hits from the large compound databases [77]. In this work, applying the SBVS approach to dock the molecules to the trimer cavity or to check feasibility of using it as a target. Ligand binding to this cavity might reduce or increase the 'bouncing spring' movement in the S protein, as observed in MD simulations (Figure 3, and Movie S1, S2). This perturbation might affect its interactions with the host cell receptor or the hinge movement of the RBD domain. The compounds that exhibit a relatively high binding affinity towards the SARS-CoV-2 spike glycoprotein trimer cavity with a binding affinity -35 to -71 kcal/mol (GBVI/WSA dG) towards the trimer cavity of the S protein recorded. From the list of ligands showing best binding, the compounds that were already proven or suggested to be / can be active against the SARS-CoV-2 virus includes (Table 1): Chitosan [53-55], Rapamycin [47-49], Everolimus (RAD001) [49], Paclitaxal [78], Ritonavir [48, 50-52], SelaMeerin (Selamectin) [79], and danoprevir [52].

Among these molecules Rapamycin and Everolimus drugs were previously identified as mTOR (mammalian target of rapamycin) inhibitors [47, 50, 80-82]. The antibacterial or antiparasitic drugs from the list are Chitosan [83] or SelaMeerin (Selamectin) [84], respectively. Paclitaxel, have been found to be previously targeting Bcl-2 and microtubule associated [85, 86]. In addition,the FDA-approved drugs that target the protease are: Ritonavir [87] and Danoprevir (ITMN-191 [88].

By docking of known drugs within the trimer cavity of S protein, the relative selectivity of the cavity suggests that the majority of drugs will have a molecular weight ≥ ~700 g/mol will show better binding affinity. Particularly, a specific class of ligands (mostly macrolide type) were found showing better fitting to the trimer cavity (Figure 4a), for example, Rapamycin [47-49], Everolimus (RAD001) [49], Paclitaxal [78], and SelaMeerin (Selamectin) [79] (Figure 4a). The intermolecular interactions

Peer-reviewed version available at J. Clin. Med. 2020, 9, 1473; doi:10.3390/jcm9051473

between the S protein and compounds, suggests that residues from all three chains (A, B, and C) forming the trimer cavity are actively involved in binding with the drugs. In addition, placement of the compounds inside the trimer cavity suggests that they make use of the pocket space (forming different conformation) to form stable interactions (Figure 4a).

Table 1. List of compounds showing best binding the compounds that were already proven or suggested to be / can be active against the SARS-CoV-2 virus, and found binding to the trimer cavity of the spike protein.*

Compounds against SARA-CoV-2	GBVI/WSA dG(kcal/mo)		Mol. Wt. g/mol	Previous Target
	Trimer cavity	RBD domain		
Chitosan [53-55]	-67.49	-37.30	161.16	Antibacterial [83]
Rapamycin (Sirolimus) [47-49]	-49.28	-25.81	914.17	mTOR [47]
Paclitaxel [78]	-45.84	-32.42	853.92	Bcl-2, Microtubule Assosiated [85, 86]
SelaMeerin (Selamectin) [79]	-44.24	-32.35	769.96	Antiparasitic [84]
Everolimus (RAD001) [49]	-41.80	0.29	958.22	mTOR [82]
Ritonavir [48, 50-52]	-37.92	-24.11	720.94	HIV Protease [87]
Danoprevir (ITMN-191) [52]	-35.09	-30.80	731.83	Proteasome, HCV, Protease [88]

*Drugs in this list are in need of further clinical validation.

As a control to evaluate the structural features or selectivity of the ligands docked to the trimer cavity of the S protein, we docked this same subset (Table 1) with the RBD domain of the viral spike protein (RBD domain; PDB ID. 6lzg [89]) that is involved in interacting with the host cell receptor; ACE2 proteins [commonly studied in ref.; 16, 26, 30, 38-42, 89, 90]. The compounds that could form a linear conformation in its structure such as the Chitosan [83, 53, 54, 55] (a linear polysaccharide; -37.29 kcal/mol) have the best binding energy for the RBD domain (Figure 4b and Table 1), whilst these same ligands can form a slightly folded shape (2d-diagram in Figure 4a) for the trimer cavity. By contrast, Everolimus [49] (a macrolide type) exhibits high affinity for the trimer pocket, and very little selectivity for the RBD domain (Table 1). Moreover, observing the placements of the ligand (Figure 4b) on the RBD domains suggest that it bindings the region, where the CR3022, a neutralizing antibody isolated from a convalescent SARS patient, interact to the the receptor-binding domain (RBD) of the SARS-CoV-2 spike protein [91].

Preprints (www.preprints.org) | NOT PEER-REVIEWED | Posted: 24 April 2020 doi:10.20944/preprints202004.0439.v1

Peer-reviewed version available at J. Clin. Med. 2020, 9, 1473; doi:10.3390/jcm9051473

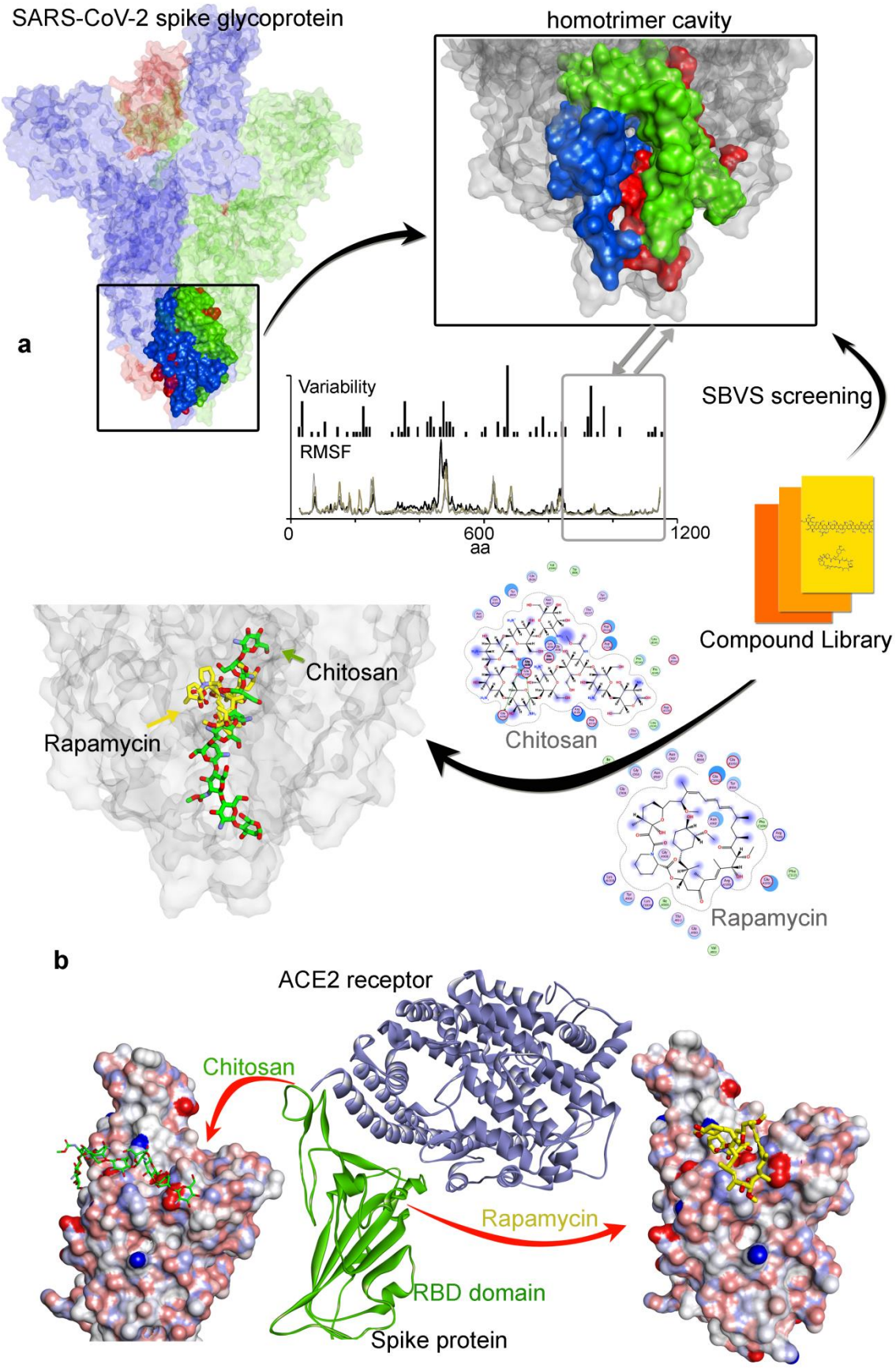

Figure 4. Targeting different pockets of the SARS-CoV-2 S protein. **(a)** The homotrimer cavity from the SARS-CoV-2 spike glycoprotein target by different compounds. **(b)** The ligands that interact with the homotrimer cavity were docked with an interface formed by spike-ACE2 proteins that interact

with ACE2 receptors. Linear form of Chitosan (a linear polysaccharide) exhibit the best binding energy with the RBD domain binding interface.

4. Discussion

The SARS-CoV-2 virus causing COVID-19 disease uses the fusion spike (S) glycoprotein to penetrate into the host cell, and therefore a detailed understanding of this protein forms a critical intervention point in the viral life-cycle. We interrogated the S protein with a diversity of computational approaches. First, the variability in S protein with respect to 791 genome viral sequences was outlined, which suggest that residues in the S2 subunit (residue range; 816-1141; HR1, CH, and CD domains) are less variable compared to other regions or domains. By contrast, residues H49Y, Q239K, V367F, V483A, S943P, K986P, and V987P are the most common amino acid substitutions in the S protein. Secondly, MD simulations revealed that the residues in RBD domain (residue range: 329-521) were more flexible compared to residues in the S2 subunit, making it more complicated for drug design strategies. An examination of less variable regions revealed that the HR1, CH and CD domains (S2 subunit) located close to the viral transmembrane formed a large cavity or pocket that is formed from three spike monomers. The MD simulation traced an 'up' active state and a 'down' inactive state of the S protein in its monomer form. Slight movement of the trimer cavity within this structural orientation suggests that it could work as 'bouncing spring' or 'sarrus linkage' when interacting with the host cell receptor.

Our investigation into the genomic variation within virus strains, as well as our findings from MD simulations of the spike protein, identified a conserved trimer cavity or pocket formed by the S2 subunit in the S protein. These findings suggest that a novel target 'the trimer cavity of S protein' may be suitable to manipulate viruses of this class. Targeting the trimer pocket might identify a new functional class of drugs against this protein. Applying the SBVS approach, we docked drug libraries against the trimer cavity with the hypothesis that such a ligand might perturb the predicted 'bouncing spring' movement and homotrimer formation. Protein-ligand docking identified several hits that have already been validated to inhibit the SARS-CoV-2 virus in cell systems. Therefore, our studies suggest an action mechanism for molecules such as Chitosan and macrolide types.

Based on the sequence variability of the Coronavirus, including our findings from MD simulations of the spike S protein, a conserved trimer cavity (HR1, CH and CD domains) is a feature of the S-protein in most Coronaviruses. Consistent with this, previous work has shown that the molecule EK1 exhibited potent inhibitory activity against all hCoVs tested through binding to the C-terminal HR1 domain [37]. Additionally, the 'up' and 'down' conformations of RBD domain observed during MD simulations, supports that concept that the S protein can also be a target of a possible IgG therapeutic [91]. From the list of the top compounds identified that dock into the trimer cavity, some of them have already been validated as SARS-CoV-2 virus inhibitors in cells, including; a Chitosan derivative [53-55], Rapamycin [47-49], Everolimus (RAD001) [49], Paclitaxal [78], Ritonavir [48, 50-52], SelaMeerin (Selamectin) [79], and Danoprevir [52]. Among these, a modified polymeric version of the Chitosan drug (a top hit in our analysis) was recently shown to inhibit CoV replication with evidence that the molecule inhibits the binding of the viral S protein to the host ACE2 receptor [53-55]. The protein-protein interaction map or the network-based methodologies [14, 43] suggest that Sirolimus (Rapamycin) emerges as a common potential drug lead for repurposing against COVID-19. This Rapamycin (mTOR inhibitor) drug was found previously to disrupt LARP1-mTORC1 binding, and has been shown to reduce MERS infection by ~60% *in vitro* [69]. The postulated geroprotectors, such as sirolimus (rapamycin) and its close derivative rapalog everolimus (RAD001), decreased infection rates in a small sample of elderly patients [49].

Moreover, the drugs Sirolimus and Ritonavir (Table 1) are currently in clinical trials for repurposing against COVID-19 [48, 50, 51]. Sirolimus is currently a registered clinical trial (NCT03901001 not yet recruiting) designed to evaluate adjunctive use of sirolimus and oseltamivir in patients hospitalized with influenza [47, 48]. Ritonavir, a HIV protease inhibitor is in open-label trial in hospitalized adults with severe COVID-19 [48, 51]. The data from this small-sample clinical study showed that danoprevir boosted by ritonavir is safe and well tolerated in all patients [52].

Selamectin is a potential drug for treating 2019-nCoV found active against the pangolin coronavirus GX_P2V, a workable model for 2019-nCoV research [79]. The antitumor drug paclitaxel increases cellular methylglyoxal to virucidal levels, providing a rationale for repurposing doxorubicin and paclitaxel for COVID-19 treatment [78]. Nevertheless, whether the ligand docking we use to identify potential mechanism(s) of action that can impact on the virus life cycle requires orthogonal systems. We hope the findings of our study can help to understand the function of the highly conserved S protein trimer cavity in the SARS-CoV-2 viral life cycle, as well as provide a novel approach to target this class of infectious disease by the examination of S protein trimer stability and/or assembly.

Supplementary Materials: The following are available online at www.mdpi.com/xxx/s1, Table S1-S3: Variability in the SARS-CoV-19 S protein for the entire sequence or specifically to RBD domain and S2 subunit domains. The amino acid substitutions in each position across 791 SARS-CoV-2 strains from the GISAID database. Table S4: The most common amino acid substitutions, the position in the chain. Figure S1 and Table S5: The intermolecular H-bond interactions formed between three chains (A-B, A-C, and B-C) of the homotrimer S protein, traced during the MD simulations. Movie S1: The conformation dynamics of the monomeric form of the S protein. Movie S2: The conformation dynamics of homotrimer S protein observed during the MD simulations, by focusing on the homotrimer cavity.

Author Contributions: Conceptualization and writing original draft: U.K., M.P., T.R.H., and J.A.A. Data curation and formal analysis: U.K., M.P., M.M, N.C., T.R.H., and J.A.A, Project administration: U.K., T.R.H., and J.A.A. Writing – review & editing: U.K., T.R.H., J.A.A., M.L., J.N., M.B., A.S, A.D, R.F., K.B., and J.H.

Funding: The APC was funded by the International Centre for Cancer Vaccine Science, University of Gdansk.

Acknowledgments: The International Centre for Cancer Vaccine Science project is carried out within the International Research Agendas programme of the Foundation for Polish Science co-financed by the European Union under the European Regional Development Fund. Authors would also like to thank the PL-Grid Infrastructure, Poland for providing their hardware and software resources.

Conflicts of Interest: The authors declare no conflict of interest.

References

1. Chan, J.F.W.; To, K.K.W.; Tse, H.; Jin, D.Y.; Yuen, K.Y. Interspecies transmission and emergence of novel viruses: lessons from bats and birds. *Trends Microbiol.* **2013,** *21*, 544-555.
2. Cheng, V.C.C.; Lau, S.K.P.; Woo, P.C.Y.; Yuen, K.Y. Severe acute respiratory syndrome coronavirus as an agent of emerging and reemerging *infection. Clin. Microbiol. Rev*. **2007**, *20*, 660-694.
3. Chan, J.F.W.; Lau, S.K.P.; To, K.K.W.; Cheng, V.C.C.; Woo, P.C.Y.; Yuen, K.Y. Middle east respiratory syndrome coronavirus: another zoonotic betacoronavirus causing SARS-like disease. *Clin. Microbiol. Rev.* **2015**, *28*, 465-522.
4. Chan, J.F.W.; Kok, K.H.; Zhu, Z.; Chu, H.; To, K.K.W.; Yuan, S.; Yuen, K.Y. Genomic characterization of the 2019 novel human-pathogenic coronavirus isolated from a patient with atypical pneumonia after visiting Wuhan. *Emerg. Microbes Infect.* **2020**, *9*, 221-236.
5. Lau, S.K.P.; Woo, P.C.Y.; Yip, C.C.Y.; Tse, H.; Tsoi, H.W.; Cheng, V.C.C.; Lee, P.; Tang, B.S.; Cheung, C.H.; Lee, R.A. et al. Coronavirus HKU1 and other coronavirus infections in Hong Kong. *J. Clin. Microbiol.* **2006**, *44*, 2063-2071.
6. Shanmugaraj, B.; Siriwattananon, K.; Wangkanont, K.; Phoolcharoen, W. Perspectives on monoclonal antibody therapy as potential therapeutic intervention for coronavirus disease-19 (COVID-19). *Asian Pac. J. Allergy Immunol.* **2020**, doi: 10.12932/ap-200220-0773
7. Zhou, H.; Chen, X.; Hu, T.; Li, J.; Song, H.; Liu, Y.; Peihan, W.; Liu, D.; Jing, Y, Edward C. H.; Alice C. et al A novel bat coronavirus reveals natural insertions at the S1/S2 cleavage site of the Spike protein and a possible recombinant origin of HCoV-19. **2020**, doi: 10.1101/2020.03.02.974139
8. Liu, Z, Xiao, X.; Wei, X.; Li, J.; Yang, J.; Tan, H.; Zhu, J.; Zhang, Q.; Wu, J.; Liu, L. Composition and divergence of coronavirus spike proteins and host ACE2 receptors predict potential intermediate hosts of SARS-CoV-2. *J. Med. Virol.* **2020**, doi: 10.1002/jmv.25726
9. Smith, R. D. Responding to global infectious disease outbreaks: Lessons from SARS on the role of risk perception, communication and management. *Soc. Sci. Med.* **2006**, *63*, 3113–3123.

10. Woo, P.C.Y.; Lau, S.K.P.; Chu, C.M.; Chan, K.H.; Tsoi, H.W.; Huang, Y.; Beatrice, H.L.W.; Rosana W.S.P.; James J.C.; Wei-kwang, L. et al. Characterization and complete genome sequence of a novel coronavirus, coronavirus HKU1, from patients with pneumonia. *J. Virol.* **2004**, *79*, 884-895.
11. Peiris, J.S.; Lai, S.T.; Poon, L.L.; Guan, Y.; Yam, L.Y.; Lim, W.; Nicholls, J.; Yee, W. K.; Yan, W. W.; Cheung, M.T.; Cheng, V.C.; et al. Coronavirus as a possible cause of severe acute respiratory syndrome. *Lancet* **2003**, *361*, 1319-1325.
12. Yeung, M.L.; Yao, Y.; Jia, L.; Chan, J.F.; Chan, K.H.; Cheung, K.F.; Chen, H.; Poon, V. K.; Tsang, A.K.; To, K K.; et al. MERS coronavirus induces apoptosis in kidney and lung by upregulating Smad7 and FGF2. *Nat. Microbiol.* **2016**, *1*, 16004.
13. Sheahan, T.P.; Sims, A.C.; Zhou, S.; Graham, R.L.; Hill, C.S.; Leist, S.R.; Alexandra, S.; Kenneth, H.D.; Stephanie, A.M.; Maria, L.A.; Andrea, J.P. et al. An orally bioavailable broad-spectrum antiviral inhibits SARS-CoV-2 and multiple endemic, epidemic and bat coronavirus. **2020**, doi: 10.1101/2020.03.19.997890
14. David, E.G.; Gwendolyn, M.J.; Mehdi, B.; Jiewei, X.; Kirsten, O.; Matthew, J.; Jeffrey Z G.; Danielle L.S.; Tia A.T.; et al. A SARS-CoV-2-Human protein-protein interaction map reveals drug targets and potential drug-repurposing. **2020**, doi: https://doi.org/10.1101/2020.03.22.002386
15. Zhang, L.; Lin, D.; Sun, X.; Curth, U.; Drosten, C.; Sauerhering, L.; Stephan, B.; Katharina, R.; Hilgenfeld, R. Crystal structure of SARS-CoV-2 main protease provides a basis for design of improved α-ketoamide inhibitors. *Science* **2020**, doi: 10.1126/science.abb3405
16. Lan, J.; Ge, J.; Yu, J.; Shan, S.; Zhou, H.; Fan, S.; Qi, Z.; Xuanling, S.; Qisheng, W.; Linqi, Z.; Wang, X. Structure of the SARS-CoV-2 spike receptor-binding domain bound to the ACE2 receptor. *Nature* **2020**, doi: 10.1038/s41586-020-2180-5
17. Tchesnokov, E.; Feng, J.; Porter, D.; Götte, M. Mechanism of inhibition of Ebola virus RNA-dependent RNA polymerase by remdesivir. *Viruses* **2019**, *11*, 326.
18. Wrapp, D.; Wang, N.; Corbett, K.S.; Goldsmith, J.A.; Hsieh, C.L.; Abiona, O.; Graham, B.S.; McLellan, J.S. Cryo-EM structure of the 2019-nCoV spike in the prefusion conformation. *Science* **2020**, 367, 1260-1263.
19. Zhou, G.; Zhao, Q. Perspectives on therapeutic neutralizing antibodies against the novel coronavirus SARS-CoV-2. *Int. J. Biol. Sci.* **2020**, *16*, 1718-1723.
20. Utomo, R.Y.; Ikawati, M.; Meiyanto, E. Revealing the potency of citrus and galangal constituents to halt SARS-CoV-2 infection. **2020**, doi: 10.20944/preprints202003.0214.v1
21. Li, F. Structure, function, and evolution of coronavirus spike proteins. *Annu. Rev. Virol.* **2016**, *3*, 237-261.
22. Bosch, B.J.; Zee, R.V.D.; Haan, C.A.M.D.; Rottier, P.J.M. The coronavirus spike protein is a Class I virus fusion protein: structural and functional characterization of the fusion core complex. *J. Virol.* **2003**, *77*, 8801-8811.
23. Ahmed, S.F.; Quadeer, A.A.; Mckay, M.R. Preliminary identification of potential vaccine targets for the COVID-19 coronavirus (SARS-CoV-2) based on SARS-CoV immunological studies. *Viruses* **2020**, *12*, 254.
24. Park, T.; Lee, S.-Y.; Kim, S.; Kim, M. J.; Kim, H. G.; Jun, S.; Seung, K.; Bum, T.K.; Park, D. Spike protein binding prediction with neutralizing antibodies of SARS-CoV-2. **2020**, doi: 10.1101/2020.02.22.951178
25. Li, W.; Moore, M.J.; Vasilieva, N.; Sui, J.; Wong, S.K.; Berne, M.A.; Somasundaran, M.; Sullivan, J.L.; Luzuriaga, K.; Greenough, T.C. et al. Angiotensin-converting enzyme 2 is a functional receptor for the SARS coronavirus. *Nature* **2003**, *426*, 450-454.
26. Hoffmann, M.; Kleine-Weber, H.; Krüger, N.; Müller, M.; Drosten, C.; Pöhlmann, S. The novel coronavirus 2019 (2019-nCoV) uses the SARS-coronavirus receptor ACE2 and the cellular protease TMPRSS2 for entry into target cells. **2020**, doi: 10.1101/2020.01.31.929042
27. Wan, Y.; Shang, J.; Graham, R.; Baric, R. S.; Li, F. Receptor Recognition by the Novel Coronavirus from Wuhan: an Analysis Based on Decade-Long Structural Studies of SARS Coronavirus. *J. Virol.* **2020**, doi: 10.1128/jvi.00127-20
28. Zhou, P.; Yang, X.L.; Wang, X.G.; Hu, B.; Zhang, L.; Zhang, W.; Si, H.R.; Zhu, Y.; Li, B.; Huang, C.L.; et al. A pneumonia outbreak associated with a new coronavirus of probable bat origin. *Nature* **2020**, *579*, 270-273.
29. Wu, A.; Niu, P.; Wang, L.; Zhou, H.; Zhao, X.; Wang, W.; Jingfeng, W.; Chengyang, J.; Xiao, D.; Xianyue, W. et al. Mutations, recombination and insertion in the evolution of 2019-nCoV. **2020**, doi: 10.1101/2020.02.29.971101
30. Yan, R.; Zhang, Y.; Guo, Y.; Xia, L.; Zhou, Q. Structural basis for the recognition of the 2019-nCoV by human ACE2. **2020**, doi: 10.1101/2020.02.19.956946

31. Walls, A.C.; Park, Y.J.; Tortorici, M.A.; Wall, A.; McGuire, A.T.; Veesler, D. Structure, function, and antigenicity of the SARS-CoV-2 Spike Glycoprotein. *Cell* **2020**, S0092-8674(20)30262-2.
32. Walls, A.C.; Tortorici, M.A.; Snijder, J.; Xiong, X.; Bosch, B.J.; Rey, F.A.; Veesler, D. Tectonic conformational changes of a coronavirus spike glycoprotein promote membrane fusion. *P. Natl. Acad. Sci. USA.* **2017**, *114*, 11157-11162.
33. Gui, M.; Song, W.; Zhou, H.; Xu, J.; Chen, S.; Xiang, Y.; Wang, X. Cryo-electron microscopy structures of the SARS-CoV spike glycoprotein reveal a prerequisite conformational state for receptor binding. *Cell Res.* **2017**, *27*, 119-129.
34. Pallesen, J.; Wang, N.; Corbett, K.S.; Wrapp, D.; Kirchdoerfer, R.N.; Turner, H.L.; Cottrell, C.A.; Becker, M.M.; Wang, L.; Shi, W. et al. Immunogenicity and structures of a rationally designed prefusion MERS-CoV spike antigen. *P. Natl. Acad. Sci.* USA, **2017**, *114*, E7348–E7357.
35. Walls, A.C.; Xiong, X.; Park, Y.J.; Tortorici, M.A.; Snijder, J.; Quispe, J.; Cameroni, E.; Gopal, R.; Dai, M.; Lanzavecchia, A.; Zambon, M. et al. Unexpected receptor functional mimicry elucidates activation of coronavirus fusion. *Cell* **2019**, *176*, 1026-1039.
36. Yuan, Y.; Cao, D.; Zhang, Y.; Ma, J.; Qi, J.; Wang, Q.; Lu, G.; Wu, Y.; Yan, J.; Shi, Y.; et al. Cryo-EM structures of MERS-CoV and SARS-CoV spike glycoproteins reveal the dynamic receptor binding domains. *Nat. Commun.* **2017**, *8*, 15092.
37. Xia, S.; Liu, M.; Wang, C.; Xu, W.; Lan, Q.; Feng, S.; Feifei, Q.; Linlin, B.; Lanying, D.; Shuwen, L. et al. Inhibition of SARS-CoV-2 infection (previously 2019-nCoV) by a highly potent pan-coronavirus fusion inhibitor targeting its spike protein that harbors a high capacity to mediate membrane fusion. **2020**, doi: 10.1101/2020.03.09.983247
38. Liu, C.; Zhou, Q.; Li, Y.; Garner, L.V.; Watkins, S.P.; Carter, L.J.; Smoot, J.; Gregg, A.C.; Daniels, A.D.; Jervey, S.; Albaiu, D. Research and development on therapeutic agents and vaccines for COVID-19 and related human coronavirus diseases. *ACS Cent. Sci.* **2020**, *6*, 315-331.
39. He, J.; Tao, H.; Yan, Y.; Huang, S.Y.; Xiao, Y. Molecular mechanism of evolution and human infection with the novel coronavirus (2019-nCoV). **2020**, doi: 10.1101/2020.02.17.952903
40. Peng, C.; Zhu, Z.; Shi, Y.; Wang, X.; Mu, K.; Yang, Y.; Xinben, Z.; Zhijian, X.; Zhu, W. Exploring the binding mechanism and accessible angle of SARS-CoV-2 spike and ACE2 by molecular dynamics simulation and free energy calculation. **2020**, doi: 10.26434/chemrxiv.11877492.v1
41. Othman, H.; Bouslama, Z.; Brandenburg, J.-T.; Rocha, J. D.; Hamdi, Y.; Ghedira, K.; Najet-Srairi, A.; Hazelhurst, S. Interaction of the spike protein RBD from SARS-CoV-2 with ACE2: similarity with SARS-CoV, hot-spot analysis and effect of the receptor polymorphism. **2020**, doi: 10.1101/2020.03.04.976027
42. Smith, M.; Smith, J.C. Repurposing therapeutics for COVID-19: supercomputer-based docking to the SARS-CoV-2 viral spike protein and viral spike protein-human ACE2 interface. **2020**, doi: 10.26434/chemrxiv.11871402.v3
43. Zhou, Y.; Hou, Y.; Shen, J.; Huang, Y.; Martin, W.; Cheng, F. Network-based drug repurposing for novel coronavirus 2019-nCoV/SARS-CoV-2. *Cell discov.* **2020**, *6*, 14.
44. Senathilake, K.; Samarakoon, S.; Tennekoon, K. Virtual screening of inhibitors against spike glycoprotein of 2019 novel corona virus: a drug repurposing approach. **2020**, doi: 10.20944/preprints202003.0042.v1
45. Gordon, C.J.; Tchesnokov, E.P.; Feng, J.Y.; Porter, D.P.; Gotte, M. The antiviral compound remdesivir potently inhibits RNA-dependent RNA polymerase from Middle East respiratory syndrome coronavirus. *J. Biol. Chem.* **2020**, doi: 10.1074/jbc.ac120.013056
46. Delmas, B.; Laude, H. Assembly of coronavirus spike protein into trimers and its role in epitope expression. *J. Virol.* **1990**, *64*, 5367-5375.
47. Kindrachuk, J.; Ork, B.; Hart, B.J.; Mazur, S.; Holbrook, M.R.; Frieman, M.B.; Traynor, D.; Johnson, R.F.; Dyall, J. et al. Antiviral potential of ERK/MAPK and PI3K/AKT/mTOR signaling modulation for Middle East respiratory syndrome coronavirus infection as identified by temporal kinome analysis. *Antimicrob. Agents Chemother.* **2015**, *59*, 1088-1099.
48. Assessment of evidence for COVID-19-Related treatments: updated 3/27/2020. available at https://www.ashp.org/Pharmacy-Practice/Resource-Centers/Coronavirus
49. Zhavoronkov, A. Geroprotective and senoremediative strategies to reduce the comorbidity, infection rates, severity, and lethality in gerophilic and gerolavic infections. *Aging* **2020**, doi: 10.18632/aging.102988

50. Faccenda, E.; Armstrong, J.F.; Harding, S.D.; Pawson, A.J.; Davies, J.A. Coronavirus information. IUPHAR/BPS Guide to Pharmacology. Retrieved from https://www.guidetopharmacology.org/coronavius.jsp
51. U.S. National Library of Medicine. Clinical Trials.gov. available at https://clinicaltrials.gov.
52. Chen, H.; Zhang, Z.; Wang, L.; Huang, Z.; Gong, F.; Li, X.; Chen, Y.; Wu, J. J. First Clinical study using HCV protease inhibitor danoprevir to treat naive and experienced COVID-19 patients. **2020**, doi: 10.1101/2020.03.22.20034041
53. Milewska, A.; Chi, Y.; Szczepanski, A.; Barreto-Duran, E.; Liu, K.; Liu, D.; Xiling, G.; Yiyue, G.; Jingxin, L.; Lunbiao, C. et al. HTCC as a highly effective polymeric inhibitor of SARS-CoV-2 and MERS-CoV. **2020**, doi: 10.1101/2020.03.29.014183
54. Milewska, A.; Kaminski, K.; Ciejka, J.; Kosowicz, K.; Zeglen, S.; Wojarski, J.; Maria, N.; Krzysztof, S.; Krzysztof P. HTCC: broad range inhibitor of coronavirus entry. *Plos One* **2016**, *11*, e0156552.
55. Milewska, A.; Ciejka, J.; Kaminski, K.; Karewicz, A.; Bielska, D.; Zeglen, S.; Karolak W, Nowakowska M, Potempa J, Bosch BJ, et al. Novel polymeric inhibitors of HCoV-NL63. *Antivir. Res.* **2013**, *97*, 112-121.
56. Elbe, S.; Buckland-Merrett, G. Data, disease and diplomacy: GISAID's innovative contribution to global health. *Global challenges (Hoboken, NJ)* **2017**, *1*, 33-46.
57. Rice, P.; Longden, I.; Bleasby, A. EMBOSS: The european molecular biology open software suite. *Trends Genet.* **2000**, *16*, 276-277.
58. Rose, P.W.; Beran, B.; Bi, C.; Bluhm, W.F.; Dimitropoulos, D.; Goodsell, D.S.; Prlic, A.; Quesada, M.; Quinn, G.B.; Westbrook, J.D.; et al. The RCSB Protein Data Bank: redesigned web site and web services. *Nucleic Acids Res.* **2011**, *39*, D392–D401.
59. Edgar R.C. MUSCLE: multiple sequence alignment with high accuracy and high throughput. *Nucleic Acids Res*. **2004**, *32*, 1792-1797.
60. Waterhouse, A.; Bertoni, M.; Bienert, S.; Studer, G.; Tauriello, G.; Gumienny, R.; Heer, F.T.; de Beer, T.; Rempfer, C.; Bordoli, L. et al. SWISS-MODEL: homology modelling of protein structures and complexes. *Nucleic Acids Res.* **2018**, *46*, W296-W303.
61. Padariya, M.; Kalathiya, U.; Houston, D.R.; Alfaro, J.A. Recognition dynamics of cancer mutations on the ERp57-Tapasin interface. *Cancers* **2020**, *12*, 737.
62. Kalathiya, U.; Padariya, M.; Pawlicka, K.; Verma, C.S.; Houston, D.; Hupp, T.R.; Alfaro, J.A. Insights into the effects of cancer associated mutations at the UPF2 and ATP-binding sites of NMD master regulator: UPF1. *Int. J. Mol. Sci.* **2019**, *20*, 5644.
63. Kalathiya, U.; Padariya, M.; Baginski, M. Structural, functional, and stability change predictions in human telomerase upon specific point mutations. *Sci. Rep.* **2019**, *9*, 8707.
64. Pronk, S.; Páll, S.; Schulz, R.; Larsson, P.; Bjelkmar, P.; Apostolov, R.; Shirts, M.R.; Smith, J.C.; Kasson, P.M.; van der Spoel, D. et al. GROMACS 4.5: a high-throughput and highly parallel open source molecular simulation toolkit. *Bioinformatics* **2013**, *29*, 845-854.
65. Bjelkmar, P.; Larsson, P.; Cuendet, M.A.; Hess, B.; Lindahl, E. Implementation of the CHARMM force field in GROMACS: analysis of protein stability effects from correction maps, virtual interaction sites, and water models. *J. Chem. Theory Comput.* **2010**, *6*, 459-466.
66. Darden, T.; York, D.; Pedersen, L. Particle mesh Ewald: AnN·log(N) method for Ewald sums in large systems. *J. Chem. Phys.* **1993**, *98*, 10089-10092.
67. Hess, B.; Bekker, H.; Berendsen, H. J. C.; Fraaije, J. G. E. M. LINCS: A linear constraint solver for molecular simulations. *J. Comput. Chem.* **1997**, *18*, 1463–1472.
68. Bussi, G.; Donadio, D.; Parrinello, M. Canonical sampling through velocity rescaling. *J. Chem. Phys.* **2007**, *126*, 014101.
69. Parrinello, M.; Rahman, A. Polymorphic transitions in single crystals: a new molecular dynamics method. *J. Appl. Phys.* **1981**, *52*, 7182-7190.
70. Gunsteren, W.F.V.; Berendsen, H.J.C. A Leap-frog algorithm for stochastic dynamics. *Mol. Simulat.* **1988**, *1*, 173-185.
71. Humphrey, W.; Dalke, A.; Schulten, K. VMD: visual molecular dynamics. *J. Mol. Graph.* **1996**, *14*, 33-38.
72. Pettersen, E.F.; Goddard, T.D.; Huang, C.C.; Couch, G.S.; Greenblatt, D.M.; Meng, E.C.; Ferrin, T.E. UCSF Chimera--A visualization system for exploratory research and analysis. *J. Comput. Chem.* **2004**, *25*, 1605-1612.

73. Kitchen, D.B.; Decornez, H.; Furr, J.R.; Bajorath, J. Docking and scoring in virtual screening for drug discovery: methods and applications. *Nat. Rev. Drug Discov.* **2004**, *3*, 935-949.
74. Molecular Operating Environment (MOE) 2011.10. Chemical Computing Group (2011) Montreal, Quebec, Canada.
75. Wojciechowski, M.; Lesyng, B. Generalized Born model: analysis, refinement, and applications to proteins. *J. Phys. Chem. B* **2004**, *108*, 18368-18376.
76. Edelsbrunner, H. The union of balls and its dual shape. *Discrete Comput. Geom.* **1995**, *13*, 415-440.
77. Lill, M. Virtual screening in drug design. In silico models for drug discovery; Kortagere, S.; Ed.; Humana Press: Totowa, NJ, USA, **2013**, *993*, 1-12.
78. Al-Motawa, M.; Abbas, H.; Wijten, P.; Fuente, A. D. L.; Xue, M.; Rabbani, N.; Thornalley, P.J. Vulnerabilities of the SARS-CoV-2 virus to proteotoxicity - opportunity for repurposed chemotherapy of COVID-19 infection. **2020**, doi: 10.1101/2020.04.07.029488
79. Fan, H.-H.; Wang, L.-Q.; Liu, W.-L.; An, X.-P.; Liu, Z.-D.; He, X.-Q.; Li-Hua, S.; Tong, Y.-G. Repurposing of clinically approved drugs for treatment of coronavirus disease 2019 in a 2019-novel coronavirus (2019-nCoV) related coronavirus model. *Chin. Med. J.* **2020**, *1*. doi: 10.1097/cm9.0000000000000797
80. Nisha, M.; Mark, A. Targeted therapy and promising novel agents for the treatment of advanced soft tissue sarcomas, *Expert Opin. Inv. Drug* **2015**, *24*, 1409-1418.
81. Squillace, R.M.; Miller, D.; Wardwell, S.D.; Wang, F.; Clackson, T.; Rivera, V.M. Synergistic activity of the mTOR inhibitor ridaforolimus and the antiandrogen bicalutamide in prostate cancer models. *Int. J. Oncol.* **2012**, *41*, 425-432.
82. Iyer, G.; Hanrahan, A.J.; Milowsky, M I.; Al-Ahmadie, H.; Scott, S.N.; Janakiraman, M.; Pirun, M.; Sander, C.; Socci, N.D.; Ostrovnaya, I. et al. Genome sequencing identifies a basis for everolimus sensitivity. *Science* **2012**, *338*, 221.
83. Kean, T.; Roth, S.; Thanou, M. Trimethylated chitosans as non-viral gene delivery vectors: Cytotoxicity and transfection efficiency. *J. Control Release* **2005**, *103*, 643-653.
84. Dryden, M.W.; Payne, P.A.; Smith, V.; Berg, T.C.; Lane, M. Efficacy of selamectin, spinosad, and spinosad/milbemycin oxime against the KS1 Ctenocephalides felis flea strain infesting dogs. *Parasites Vector.* **2013**, *6*, 80.
85. Aldonza, M.; Ku, J.; Hong, J. Y.; Kim, D.; Yu, S. J.; Lee, M. S.; Prayogo, M. C.; Tan, S.; Kim, D.; Han, J.; et al. Prior acquired resistance to paclitaxel relays diverse EGFR-targeted therapy persistence mechanisms. *Sci. Adv.* **2020**, *6*, eaav7416.
86. Ferlini, C.; Cicchillitti, L.; Raspaglio, G.; Bartollino, S.; Cimitan, S.; Bertucci, C.; Mozzetti, S.; Gallo, D.; Persico, M.; Fattorusso, C.; et al. Paclitaxel Directly Binds to Bcl-2 and Functionally Mimics Activity of Nur77. *Cancer Res.* **2009**, *69*, 6906-6914.
87. Zeldin, R. K. Pharmacological and therapeutic properties of ritonavir-boosted protease inhibitor therapy in HIV-infected patients. *J. Antimicrob. Chemother.* **2003**, *53*, 4-9.
88. Deutsch, M.; Papatheodoridis, G.V. Danoprevir, a small-molecule NS3/4A protease inhibitor for the potential oral treatment of HCV infection. *Curr. Opin. Investig. Drugs* **2010**, *11*, 951-963.
89. Zhang, G.; Pomplun, S.; Loftis, A.R.; Loas, A.; Pentelute, B.L. The first-in-class peptide binder to the SARS-CoV-2 spike protein. **2020**, doi: 10.1101/2020.03.19.999318
90. Shang, J.; Ye, G.; Shi, K.; Wan, Y.; Luo, C.; Aihara, H.; Qibin, G.; Ashley, A.; Li, F. Structural basis of receptor recognition by SARS-CoV-2. *Nature* **2020**, doi: 10.1038/s41586-020-2179-y
91. Yuan, M.; Wu, N.C.; Zhu, X.; Lee, C.CD.; So, R.T.Y.; Lv, H.; Chris, K.P.M.; Wilson, I.A. A highly conserved cryptic epitope in the receptor-binding domains of SARS-CoV-2 and SARS-CoV. *Science* **2020**, doi: 10.1126/science.abb7269